JMEPEG (2012) 21:1431–1439
DOI: 10.1007/s11665-011-0014-1

1059-9495/$19.00

The Estimation of Localized Corrosion Behavior of Ni-Based Dental Alloys Using Electrochemical Techniques

Daniel Mareci, Romeu Chelariu, Sorin Iacoban, Corneliu Munteanu, Georgiana Bolat, and Daniel Sutiman

(Submitted February 11, 2011; in revised form June 17, 2011)

The aim of this study is to investigate the electrochemical behavior of the five non-precious Ni-based dental casting alloys in acidified artificial saliva. For comparison, nickel was also investigated. In order to study the localized corrosion resistance, the cyclic potentiodynamic polarization (CCP) and electrochemical impedance spectroscopy were performed. Scanning electron microscopy (SEM) observations were made after the CCP tests. The Ni-Cr alloys with chromium (14-18%) contents were susceptible to localized corrosion. The Ni-Cr-Mo alloy with contents of chromium (≈13%) and molybdenum (9%) presents a dangerous breakdown, but have *a zero corrosion potential* so that the difference between them is around 650 mV. The Ni-Cr-Mo alloys with higher chromium (22-25%) and molybdenum (9-11%) contents had a much larger passive range in the polarization curve and were immune to pitting corrosion. Pitting resistance equivalent (PRE) of about ≈54 could provide the Ni-based alloy with a good pitting corrosion resistance.

Keywords corrosion current, EIS, localized corrosion, Ni-based alloys, potentiodynamic polarization curves

1. Introduction

There is a huge demand for metallic materials in medical devices (Ref 1). Metals and alloys are widely used as biomedical materials and are indispensable in the medical field. Metallic materials play an essential role in repair or replacement of the diseased or damaged bone tissue. However, the main limitation of these metallic materials is the release of the toxic metallic ions can lead to various adverse tissue reactions and/or hypersensitivity reactions (Ref 2). The high costs of precious metals and alloys have led to the development of various base-alloy materials, which are more economical. The most important components of these alloys are titanium, nickel, cobalt, chromium, copper, and iron (Ref 3, 4). The selection is made depending not only on the mechanical and biocompatibility properties but also on the corrosion resistance of the alloy and is dependent on the clinical case. The Ni-based alloys are the most commonly used metal-based alloys in dentistry. There is a wide variety of commercially available Ni-based dental alloys. In the actual socio-economical conditions, the dental physician should select with discernment the alternatives to Ni-based alloys, existing currently in the world market. These materials are currently used for crowns, bridges casting and denture bases. Ni-based alloys are commonly used as the substructure of metallic-ceramic crown and were introduced into dentistry as possible replacement for precious alloys (Ref 4-6). Ni-based alloys offer the advantage of an increased Young's modulus (around 200 GPa) compared with gold (around 100 GPa) and this advantage allows for thinner sections of alloy to be used and consequently less tooth destruction during the crown preparation (Ref 5, 7).

The primary alloying element with the Ni-base alloys is chromium that is added to promote the formation of a stable passive oxide layer that is highly resistant to corrosion (Ref 1). Molybdenum is also frequently added to promote resistance to pitting and crevice corrosion (Ref 8, 9). Elements such as beryllium (highly toxic), niobium, iron, aluminium, copper, and manganese can also be added, but chromium and molybdenum are added for corrosion resistance. Ameer et al. (Ref 10), Mareci et al. (Ref 11) and Sharma et al. (Ref 12) suggest that Ni-Cr-Mo alloys have high very corrosion resistance in artificial saliva. Recently, Saji and Choe (Ref 13) reported that, on a study of preferential dissolution behavior in Ni-Cr dental cast alloy, this alloy presented a dangerous breakdown potential of around 150 mV.

The presence of crevices combined with an inhomogeneous distribution of chromium in the microstructure can lead to the corrosion of Ni-based alloys with lower chromium contents. This effect can be avoided by increasing the chromium content of the alloy (Ref 5).

Nickel is an allergen, but there is no evidence that individual patients are at a significant risk of developing sensitivity solely due the contact with Ni-based dental appliances and restorations. It has been reported that the corrosion products from Ni-Cr based alloys do not affect cellular morphology or viability but that they

Daniel Mareci, Georgiana Bolat, and **Daniel Sutiman**, Faculty of Chemical Engineering and Environmental Protection, "Gheorghe Asachi" Technical University of Iasi, 73 Prof. dr. doc. D. Mangeron Blvd., 700050 Iasi, Romania; **Romeu Chelariu**, Faculty of Materials Science and Engineering, "Gheorghe Asachi" Technical University of Iasi, 61A Prof. dr. doc. D. Mangeron Blvd., 700050 Iasi, Romania; and **Sorin Iacoban** and **Corneliu Munteanu**, Faculty of Mechanical Engineering, "Gheorghe Asachi" Technical University of Iasi, 61-63 Prof. dr. doc. D. Mangeron Blvd., 700050 Iasi, Romania. Contact e-mail: georgiana20022@yahoo.com.

do decrease cellular proliferation (Ref 14). The metal ions released from Ni-Cr-based dental casting alloys interfere with cellular energy metabolism (Ref 15). However, nickel has the ability to bind to oxygen, nitrogen, and sulfur from bio-compounds, replacing the usual catalysts (magnesium and calcium) which are essential in many metabolic activities.

Previous study (Ref 16) has highlighted that Ni-ion release from Ni-Cr alloys after 30 days immersed in artificial saliva are small (1-6 ppm).

Though the allergic properties of the metal ions of Ni-Cr alloys should be considered carefully, these alloys still remain very popular for dental use. Hypersensitivity reactions to nickel are only likely to occur with prior sensitization from non-dental contacts, and even these are rare (Ref 17).

The electrochemical behavior of a dental alloy in artificial saliva permits the estimation of the behavior of the material in the oral cavity. The modifications of the dental alloys properties could be determined using rapid electrochemical tests as a qualitative criterion to estimate the corrosion parameters.

The present article made a comparative study of the Ni-based dental casting alloys with different compositions on the susceptibility to localized corrosion (pitting and crevice corrosion) in artificial saliva. For comparison, nickel was also investigated.

2. Materials and Methods

2.1 Materials and Sample Preparation

Five non-precious Ni-based dental casting alloys used in dental prosthetics construction were investigated. The names and chemical compositions of the alloys are shown in Table 1. For comparison, nickel (99.7 wt.%, The British Drug Houses LTD, B.D.H. Laboratory Chemicals Group, UK) was also investigated.

The tests specimens were embedded in a polytetrafluoroethylene (PTFE) holder specifically designed to connect to a rotating disk electrode (RDE) (type EDI 101T; Radiometer Analytical). A polymeric resin was used to ensure a tight seal between the alloy specimen and the PTFE holder, as shown in Fig. 1, to avoid crevice corrosion. Before corrosion tests and surface examination, the electrodes were wet-polished with 250, 400, 600, 1000, and 2500 grit metallographic abrasive papers, and final polishing was done with 1 μm alumina suspension. The samples were degreased with ethyl alcohol, followed by ultrasonic cleaning with deionized water.

In all the measurements, the surface area of the samples consisting of RDE electrode was 0.19 cm^2.

2.2 Test Corrosion Medium

Human artificial saliva can vary to a considerable degree and is dependent on the age and sex of the patient, the time of day, eating habits, medication, and oral hygiene (Ref 18). In the present study, Fusayama's artificial saliva was selected as it has been shown to produce results that were consistent with the clinical experience of dental alloys (Ref 19). Fresh Fusayama's artificial saliva (Ref 20) as corrosion medium was prepared before use. It is composed of 0.400 g NaCl; 0.400 g KCl; 0.795 g $CaCl_2{\cdot}2H_2O$; 0.780 g $NaH_2PO_4{\cdot}2H_2O$; 0.005 g $Na_2S{\cdot}9H_2O$; 1.000 g NH_2CONH_2, and distilled water up to 1000 mL. The pH of such solution is about 5.6. Because the short-term pH variances include the intake of acidic beverages (pH 2-3) and secretion of gastric acid (pH 1), we added lactic acid to the Fusayama's artificial saliva to decrease the pH to 2.3 to accentuate corrosion.

2.3 Electrochemical Measurements

The tests specimens was placed in a glass corrosion cell, which was filled with freshly prepared electrolyte. A saturated calomel electrode (SCE) was used as the reference electrode and a platinum coil as the counter electrode. All potentials referred to in this article are with respect to SCE. A rotation speed of 500 rpm for the RDE was used for keeping the solution homogenous throughout the test.

All the electrochemical measurements were performed with a PAR (Princeton Applied Research, USA) 263 A potentiostat connected with a PAR 5210 lock-in amplifier controlled by a personal computer and specific software (Electrochemistry Power Suite, PAR).

For all the samples, 2-h open-circuit potential (E_{OC}) measurement was performed initially followed by the CCP

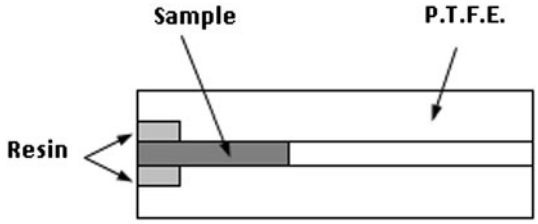

Fig. 1 Rotating disk electrode

Table 1 Chemical composition of the investigated Ni-based dental casting alloys

	Element, wt.%									
Name of dental alloys	**Cr**	**Mo**	**Be**	**Mn**	**Cu**	**Al**	**Fe**	**Si**	**Nb**	**Ni**
NicromalSoft	17.8	…	…	3.5	9.8	1.5	0.5	1.8	…	Bal
VeraSoft	14.5	…	…	19.5	9.5	1.6	…	1.5	…	Bal
Gialloy	25	11	…	…	…	…	…	1.5	…	Bal
Wiron99	22.5	9.5	…	…	…	…	0.5	1	1	Bal
VeraBondV	12.7	9	1.95	…	…	2	…	…	…	Bal

According to the data provided by the manufacturer; NicromalSoft: I.M.N.R., Romania; VeraSoftand and VeraBondV: Aalba Dent Inc., USA; BK Giulini, Germany; Wiron99: Bego, Germany

measurement. These tests were conducted by stepping the potential using a scanning rate of 0.5 mV/s from −600 mV (SCE) to +1200 mV (SCE) and then reversed to −500 mV (SCE). Using an automatic data acquisition system, the CCP curves were plotted, and both the corrosion current density (i_{corr}) and the zero current potential (ZCP) were estimated. For evaluating the stability of passivation, passivation current density (i_{pass}), breakdown potential (E_{bd}), and repassivation potential (E_{rp}) were obtained from the CCP curves.

Electrochemical impedance spectroscopy (EIS) was also used in this study. The alternating current (AC) impedance spectra for VeraBondV alloy was obtained with a scan frequency ranging from 100 kHz to 10 mHz with an amplitude of 10 mV. The EIS spectra were obtained at different times and different potentials after the electrode was immersed in the aerated artificial saliva. In order to supply quantitative support for discussions of these experimental EIS results, an appropriate model (ZSimpWin-PAR, USA) for equivalent circuit (EC) quantification has also been used. The EC consists of various arrangements of resistances, capacitors, and other circuit elements, and provides the most relevant corrosion parameters applicable to the substrate/electrolyte system. The usual guidelines for the selection of the best-fit EC were followed: a minimum number of circuit elements are employed so that the χ^2 error was suitably low ($\chi^2 < 10^{-4}$), and the error associated with each element was up to 5%. Instead of pure capacitors, constant phase elements (CPEs) were introduced in the fitting procedure to obtain good agreement between the simulated and experimental data.

The impedance of the CPE is given by (Ref 6):

$$Q = Z_{CPE} = \frac{1}{C(j\omega)^n} \quad \text{(Eq 1)}$$

where, for $n = 1$, the Q element reduces to a capacitor with a capacitance C and, for $n = 0$, to a simple resistor. n is related to a slope of the log Z_{mod} vs. log Frequency Bode-plots, ω is the angular frequency, and j is imaginary number ($j^2 = -1$).

All the polarization experiments were performed three times. These replications were not sufficient for carrying out statistical analysis but served to verify the reproducibility of the results obtained.

2.4 SEM Microscopy of Corroded Surfaces

The surface morphology modifications as a result of the corrosion processes were analyzed by scanning electron microscopy (SEM) microscopy, using a SEM VEGA II LSH manufactured by Tescan Co. (Czech Republic) coupled with an EDX QUANTAX QX 2 detector manufactured by Bruker/Roentec Co. (Germany).

3. Results and Discussions

The intra-orally temperature widely fluctuates because of ingestion of hot or cold food and beverage. Furthermore, different areas of oral cavity exhibited different temperatures. Nevertheless, it can be reasonably approximated in experimental settings if we considered the environmental temperature as 25 °C (Ref 21).

For a specific environment, corrosion depends on the structure and chemical composition of the alloy. The alloys of the present study have different chemical compositions and microstructure. The microstructural characterization of the Ni-based alloys was detailed elsewhere (Ref 11, 22).

The CCP curves in a semi-logarithmic version of the pure nickel, Ni-Cr alloys, and Ni-Cr-Mo alloys after 2-h immersion in acidified artificial saliva at 25 °C are displayed in Fig. 2-4. PowerCorr software (PAR, USA) was employed to extract ZCP

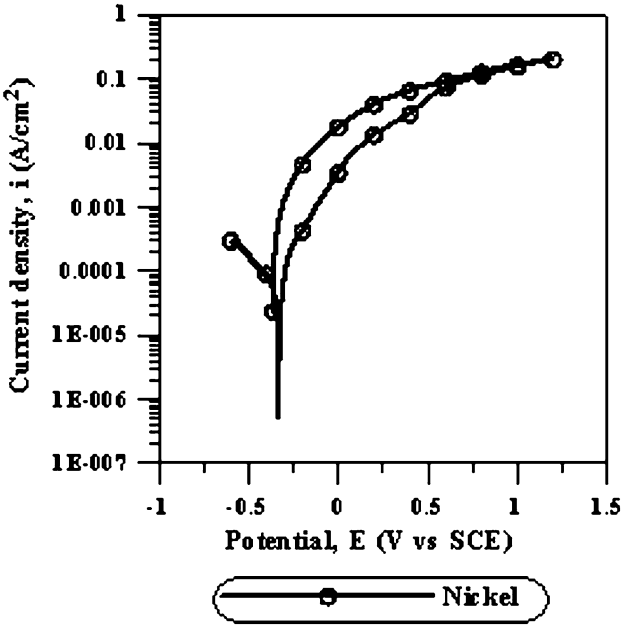

Fig. 2 Cyclic potentiodynamic polarization curves in semi-logarithmic coordinates for nickel tested after 2 h of immersion in acidified artificial saliva, at 25 °C

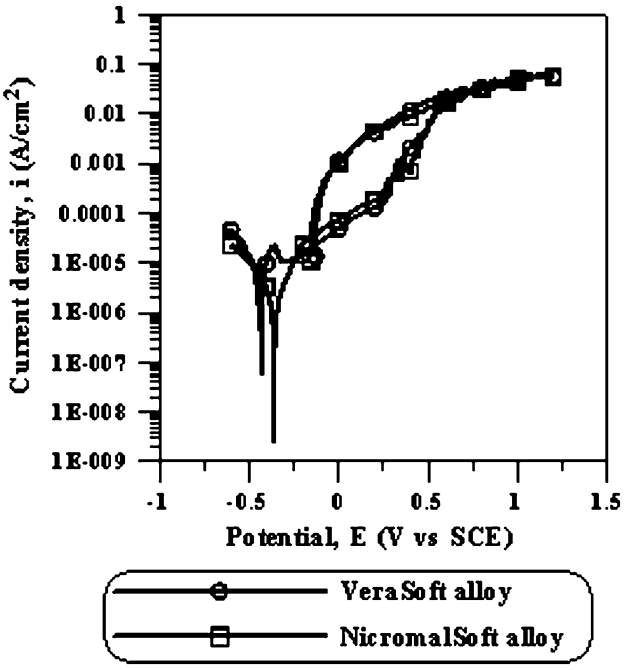

Fig. 3 Cyclic potentiodynamic polarization curves of Ni-Cr alloys tested after 2 h of immersion in acidified artificial saliva, at 25 °C, on semi-logarithmic coordinates

and corrosion current (i_{corr}) values from the potentiodynamic polarization plots. The average ZCP and i_{corr} from polarization curves determined by the program software are presented in Table 2.

The ZCP is defined as the potential at which the current reaches a minimum during the forward potentiodynamic polarization scan. The corrosion current (i_{corr}) is representative for the degradation degree of the alloy.

In the case of nickel (Fig. 2), the sharp increases of the anodic current indicate a metallic dissolution, an active state. The corrosion current density of nickel was around 90 μA/cm^2.

The two Ni-Cr alloys (VeraSoft and NicromalSoft alloys) in acidified artificial saliva exhibited similar polarization curves. The corrosion resistance (decreasing the corrosion current density) of the Ni-Cr alloys is improved by the chromium content. It has been reported that chromium-containing Ni-based alloys in acid solutions become passive by anodic polarization (Ref 23). However, the oxide film is not considered to be an efficient barrier to dissolution, because the anodic current shows a monotonical increase near the ZCP. On the other hand, the two Ni-Cr alloys show a large positive hysteresis because of being susceptible to pitting corrosion (Fig. 3). The area of hysteresis loop is a direct measure of the pits propagation kinetics.

In the case of Ni-Cr-Mo alloys (Fig. 4), all materials translated directly into a stable passive behavior from the "Tafel region" without exhibiting a traditional active-passive transition. In this study, the Gialloy and Wiron99 specimens showed no positive hysteresis loop in the polarization curve.

The susceptibility of an alloy to pitting corrosion and crevice corrosion in a certain medium can be characterized in terms of the breakdown potential (E_{bd}) and repassivation potential (E_{rp}), relative to the ZCP (Ref 24-26). E_{br} is defined by the intersection of a tangent to the anodic branch of the polarization curve with the potential axis at zero current, where the polarization curve starts to increase steeply in positive value. It marks the point beyond which degradation becomes massive. The E_{rp} is observed where the reverse scan branch (cathodic branch) intersects the anodic branch. Between E_{rp} and E_{bd}, old pits (or pre-existing pits) can grow, but new surface pits cannot make their beginning. The new pits begin only when the potential is above E_{bd}. The potential range situated between the ZCP and E_{bd} represents the passivity zone in which corrosion is weak or even insignificant. Thus, the difference between the E_{bd} and the ZCP is commonly used as a measure of the alloy's susceptibility to pitting corrosion. The difference between the E_{rp} and ZCP reflects the susceptibility to crevice corrosion. As the difference between, E_{bd} and ZCP becomes smaller, the alloy is expected to become more susceptible to pitting corrosion. If ZCP is similar to or is more positive than E_{rp}, then the alloy is likely to undergo pitting attack in the stationary condition (case of nickel).

Table 2 lists the values of breakdown potential (E_{bd}), and repassivation (E_{rp}) together with values calculated for E_{bd} − ZCP and E_{rp} − ZCP. According to the values of E_{bd}, this quite a different corrosion behavior can be attributed to Ni-Cr-Mo alloys. E_{bd} of VeraBondV alloy is around 150 mV. The passive zone is around 650 mV (E_{bd} − ZCP), implying the corrosion start from 150 mV and is susceptible to crevice corrosion (E_{rp} − ZCP is small, around 235 mV). E_{bd} of Gialloy is around 650 mV, and the passive zone is very large. The passive zone of the Gialloy alloy extends up to 1100 mV. The Wiron99 alloy presents a similar behavior, with E_{bd} at around 700 mV and the passive zone at around 1100 mV.

The low Cr and Mo contents in the Ni-based alloys are associated with a high corrosion rate and susceptibility to accelerated corrosion processes (Ref 27). In this study, the presence of the larger passive range for the Gialloy and

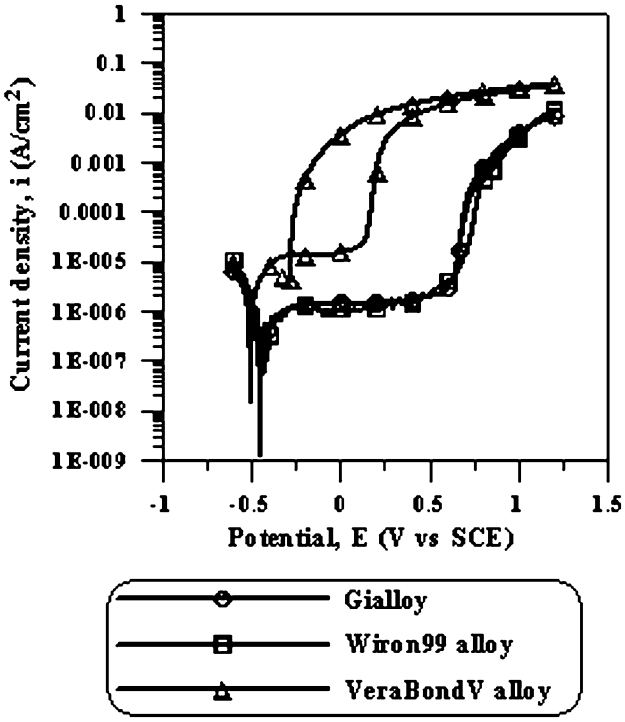

Fig. 4 Cyclic potentiodynamic polarization curves of Ni-Cr-Mo alloys tested after 2 h of immersion in acidified artificial saliva, at 25 °C, on semi-logarithmic coordinates

Table 2 The mean and standard deviation values of parameters measured and calculated for the various Ni-based alloys in acidified artificial saliva (25 °C)

Alloy	ZCP, mV	i_{corr}, μA/cm^2	i_{pass}, μA/cm^2	E_{bd}, mV	E_{rp}, mV	E_{bd} − ZCP, mV	E_{rp} − ZCP, mV
Nickel	−320 ± 8	90 ± 3	…	…	…	…	…
NicromalSoft	−350 ± 16	10.5 ± 0.2	…	…	…	…	…
VeraSoft	−425 ± 15	16.5 ± 0.3	…	…	…	…	…
VeraBondV	−510 ± 8	6.0 ± 0.2	12.5 ± 0.4	140 ± 6	−275 ± 4	650 ± 7	235 ± 6
Gialloy	−440 ± 12	0.9 ± 0.1	1.5 ± 0.1	670 ± 11	…	1110 ± 11	…
Wiron99	−435 ± 11	1.1 ± 0.1	1.4 ± 0.1	710 ± 13	…	1145 ± 12	…

ZCP, zero current potential; i_{corr}, corrosion current density; i_{pass}, passive current density; E_{bd}, breakdown potential; E_{rp}, repassivation potential

Wiron99 specimens with respect to the other three Ni-based alloys was ascribed mainly to higher amounts of Cr and Mo in the chemical composition of specimens.

Passive current density (i_{pass}) was also determined from the potentiodynamic anodic diagram and is obtained around the middle of the passive range. Passive current densities are listed in Table 2. The passive current densities of the Gialloy and Wiron99 are small, of around of 1-2 μA/cm^2. The passive current densities for VeraBondV samples are approximately ten times higher than those in the case of Gialloy and Wiron99 samples. It is well known that if the metal shows lower i_{pass} with longer potential range, the metal is considered to possess a better and more stable passivity.

Figure 5 shows the corroded surfaces of the four alloys, VeraSoft, Gialloy, Wiron99, and VeraBondV, after CCP experiments were performed at 25 °C in acidified artificial saliva. The SEM images, analysis indicated a different behavior of Gialloy and Wiron99 alloys in comparison with the other two alloys characterized by localized corrosion.

The analysis of Fig. 5 indicates the appearance of localized corrosion at the surface of VeraBondV and VeraSoft alloys and the development of a uniform corrosion process in case of Gialloy and Wiron99 alloys. The localized corrosion at the surface of VeraBondV and VeraSoft alloys is evident; however, the morphology of the attack is extremely irregular. On the other hand, the EDX analysis for VeraSoft and VeraBondV alloys revealed that the black areas were richer in nickel and less rich in chromium for VeraSoft alloy, and less rich in chromium and molybdenum for VeraBondV alloy.

It has been reported that the contents of chromium and molybdenum play an important role in the corrosion resistance of Ni-based dental alloy (Ref 27-30). The presence of higher chromium (22.5-25 wt.%) and molybdenum (9.5-11 wt.%) contents in the Gialloy and Wiron99 alloy promoted immunity to pitting corrosion. The specimens without molybdenum contents (VeraSoft and NicromalSoft alloys) are susceptible to pitting corrosion. On the other hand, the VeraBondV alloy with 9% molybdenum and 12.7% chromium contents indicated a pitting corrosion after electrochemical test. For Fe-Ni-Cr-Mo stainless steel, the relative effectiveness of chromium and molybdenum contents on pitting or crevice corrosion usually can be assessed qualitatively by pitting resistance equivalent (PRE), which is represented by the empirical equation (Ref 31):

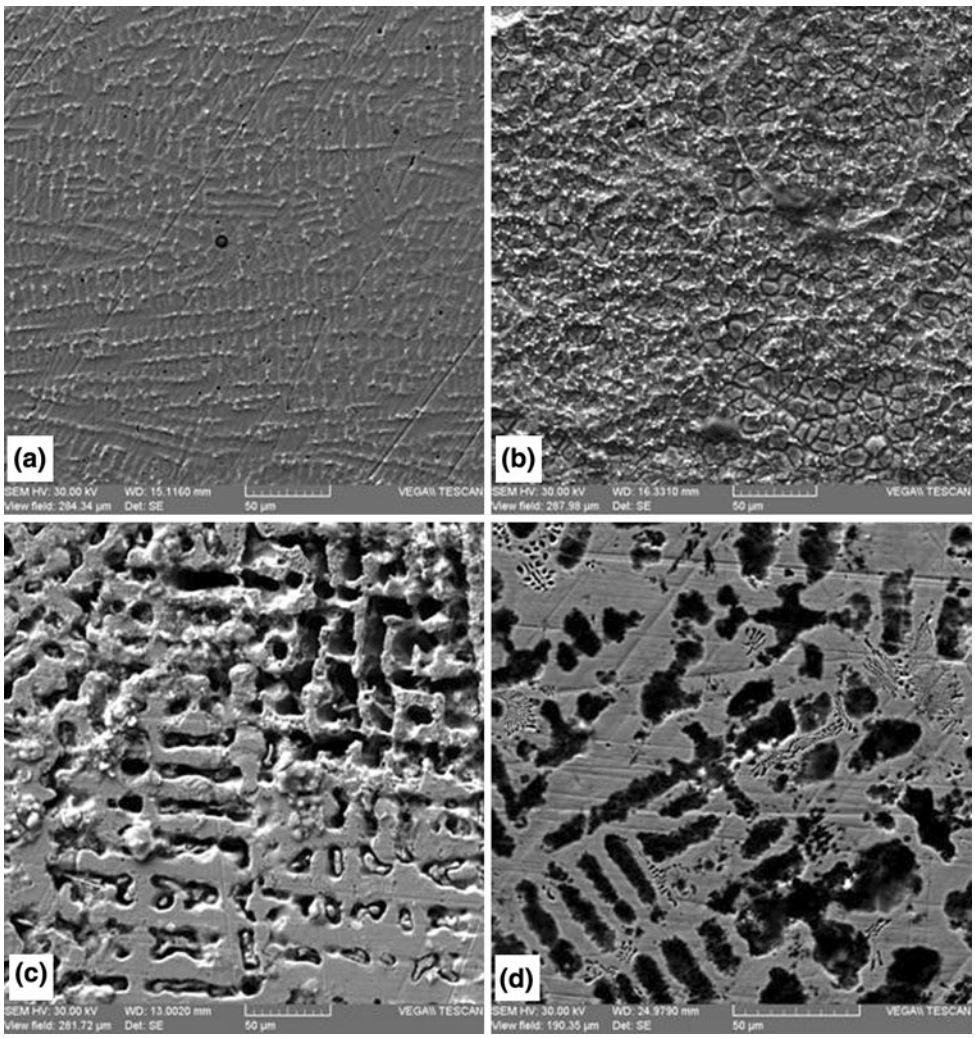

Fig. 5 Surface attack morphology: (a) Gialloy, (b) Wiron99 alloy, (c) VeraSoft alloy, (d) VeraBondV alloy

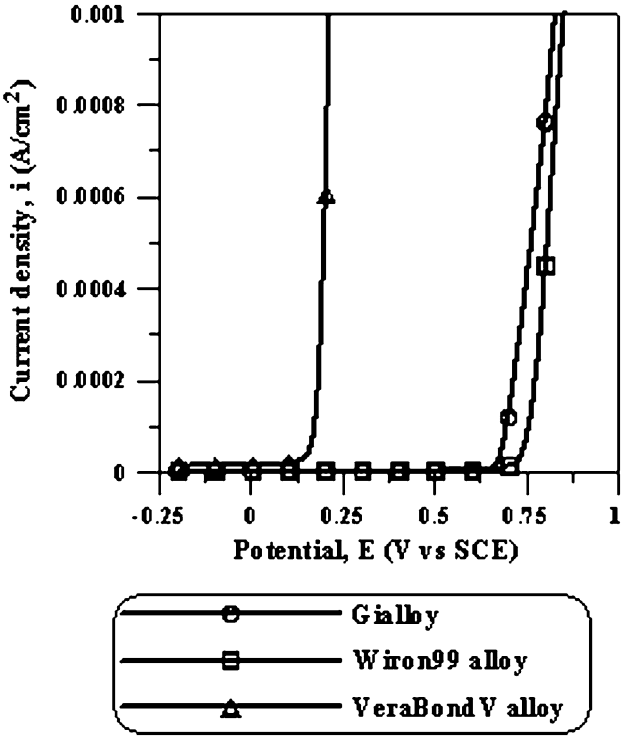

Fig. 6 The Part of polarization curve in linear representation for all the three Ni-Cr-Mo alloys after 2 h in test solution, in the scale of anodic currents comprising between 0 and 1 mA/cm^2. Potentiodynamic polarization curves presented on linear axes in order to reveal the breakdown potential for Ni-Cr-Mo alloys after 2 h in acidified artificial saliva, at 25 °C

$$\mathrm{PRE} = \%\mathrm{Cr} + 3.3\%\mathrm{Mo}$$

The Ni-Cr-Mo casting alloy is pitting resistant in acidic artificial saliva when the PRE value increases up to around 49 (Ref 31). In this study, according to the PRE equation mentioned above, the PRE values for the pitting-resistant Gialloy and Wiron99 alloys were 61.3 and 53.9, respectively. The other three alloys, which were susceptible to pitting corrosion, had PRE values between 14.5 (VeraSoft) and 42.4 (VeraBondV).

According to Fig. 3, 4, 6, the Ni-based alloys can be put into three groups. A first group with Gialloy and Wiron99 shows the best behavior, with small anodic currents and a large passive zone. VeraBondV alloy shows that anodic currents are 10 times higher with a passive zone around 650 mV, a susceptibility to crevice and pitting corrosion. A third group made up of VeraSoft and VeraBond alloys shows the worst behavior.

The VeraBondV alloy presented a small breakdown potential (E_{bd}). These potentials, however, are not specific to a particular alloy, and hence, do not allow for variations in ZCP. The values of $E_{bd} - \mathrm{ZCP}$ provide a more reliable measure of the breakdown resistance. It is known that metallic biomaterials in the human body may be exposed to potentials of up to 400 mV/SCE (Ref 32). An alloy with a particular surface condition may exhibit E_{bd} values below 400 mV/SCE, but have a ZCP such that the difference between them is higher. Table 2 shows that VeraBondV alloy in acidified artificial saliva has an E_{bd} value, of around 140 mV, but its value of $E_{bd} - \mathrm{ZCP}$ is well over 600 mV.

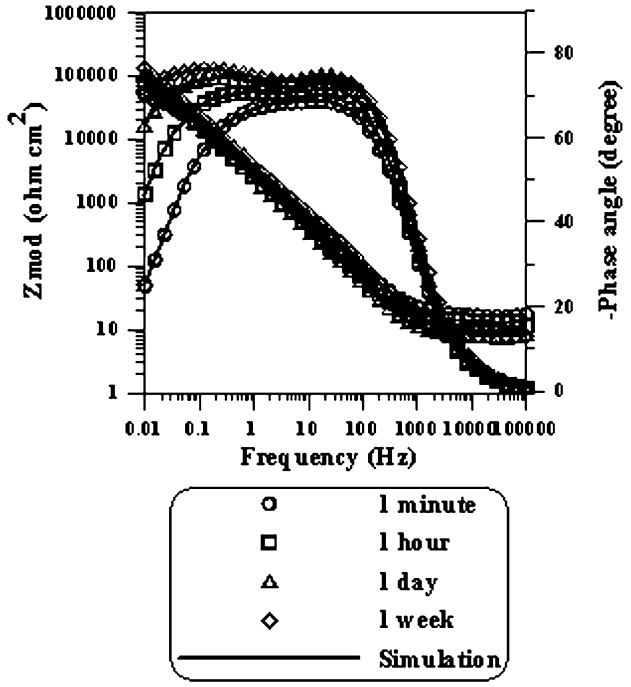

Fig. 7 Impedance spectra of VeraBondV alloy maintained different time periods in acidified artificial saliva measured at E_{OC}

A comparative study for the localized corrosion resistance of the VeraBondV alloy has been investigated in acidified artificial saliva using electrochemical impedance spectroscopy (EIS) techniques. The EIS study was performed to confirm the results obtained by the polarization tests. The EIS were performed in a wide range of potentials covering open-circuit potential (E_{OC}), passive region, and breakdown region.

The Bode spectra for the VeraBondV alloy recorded at 25 °C in acidified artificial saliva after 1 min, 1-h, 1-day, and 1-week immersions are shown in Fig. 7.

The impedance of VeraBondV alloys increases with the time of electrode immersion. All the spectra show that in a higher-frequency region, log Z_{mod} tends to become constant with a phase angle value of 0°. This is a typical response for the resistive behavior and corresponds to the solution resistance, R_{sol}. In the medium-frequency range, a linear relationship between log Z_{mod} and log Frequency is observed, but with different slopes (always less than -1) and phase angle maximum (less than $-90°$), indicating that the passive films were not fully capacitive. At intermediate frequency, the phase angle shifted to -70 for the alloy maintained 1 min in test solution and increases in time up to $-75°$ for alloy maintained 1 week in test solution. The Bode-phase plots show two time constants in all the cases.

The impedance spectra fitting for VeraBondV alloy at different time immersion in acidified artificial saliva was carried out using an EC (Fig. 8a) with a series combination of the R_{sol} solution resistance, and with two RQ elements in parallel: $R_{sol}(Q_1(R_1(R_2Q_2)))$. A very good agreement between the simulated and the experimental data was obtained. The $R_{sol}(R_1Q_1)$ model failed to provide a satisfactory fit (the values of the chi-square (χ^2) test were about 2×10^{-2}). Table 3 shows the results of the fittings. The high-frequency R_1 and Q_1 parameters are the properties of the reactions at the passive layer/solution interfaces.

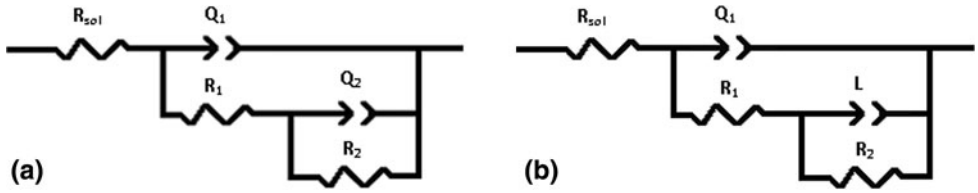

Fig. 8 Equivalent circuits (EC) used in the generation of simulated data

Table 3 Impedance parameters of VeraBondV alloy after different time immersion in acidified artificial saliva at E_{OC} (25 °C)

Immersion time	R_1, Ω cm^2	Q_1, S/cm^2 s^n	n_1	R_2, Ω cm^2	Q_2, S/cm^2 s^n	n_2
1 min	7×10^3	2.8×10^{-5}	0.86	4.6×10^4	2.3×10^{-5}	0.80
1 h	16×10^3	2.1×10^{-5}	0.87	7.8×10^4	2.1×10^{-5}	0.81
1 day	18×10^3	1.9×10^{-5}	0.87	9.8×10^4	1.7×10^{-5}	0.82
1 week	19×10^3	1.8×10^{-5}	0.88	11×10^4	1.4×10^{-5}	0.82

The R_2 and Q_2 parameters describe the properties for passive layer.

In Fig. 7, the experimental data are shown as individual points, while the theoretical spectra resulting from the fits with a relevant EC model are shown as lines.

The same value for R_{sol}, equal to 15 ± 2 Ω, was observed for VeraBondV alloy at different times of immersion.

R_1, representing the charge transfer resistance (R_{ct}), and Q_1, the double-layer capacitance, are shown by the high value of the n_1 exponent. The double layer capacitances for all the samples are typical for the C_{dl} of the passive oxide layers (Ref 33-36).

Corrosion products (passive oxide film) can block the access of electrochemically active species to the electrode surface, restricting ion diffusion to the surface, and thus reducing the overall corrosion reaction rate (Ref 37) which can explain the increase in R_2 with increasing immersion time. R_1 also increases with immersion time as more of the surface becomes covered by oxide film.

The polarization resistance (R_p) of the VeraBondV alloy equals the sum of the R_1 (R_{ct}) and the passive film resistance, R_2. R_p allows a quantitative analysis based on the specific magnitudes of the corrosion rate. It is therefore representative of the degree of protection of the passive layer at the alloy surface. A high polarization resistance value is an indication of the working electrode strongly resisting change from its equilibrium state and is representative of the degree of protection of the passivation layer of the alloy surface. The more the value of polarization resistance increases, the more the alloy will resist corrosion.

The polarization resistance (R_p) of the alloy in artificial saliva after 1-day and 1-week immersion times are the largest. For highly corrosion-resistant materials, the R_p may even reach 1 MΩ cm^2 (Ref 38).

The EIS measurements show that the passive film formed on the surface of VeraBondV alloys in acidified artificial saliva has a good stability. VeraBondV alloy exhibit a dangerous E_{bd} value below 150 mV, but have a sufficiently negative ZCP such that the difference between them is around 650 mV.

Figure 9 shows the impedance spectra of VeraBondV polarized for 30 min in artificial saliva at −250 mV (in passive zone, but more positive than repassivation potential) and at 145 mV (breakdown potential).

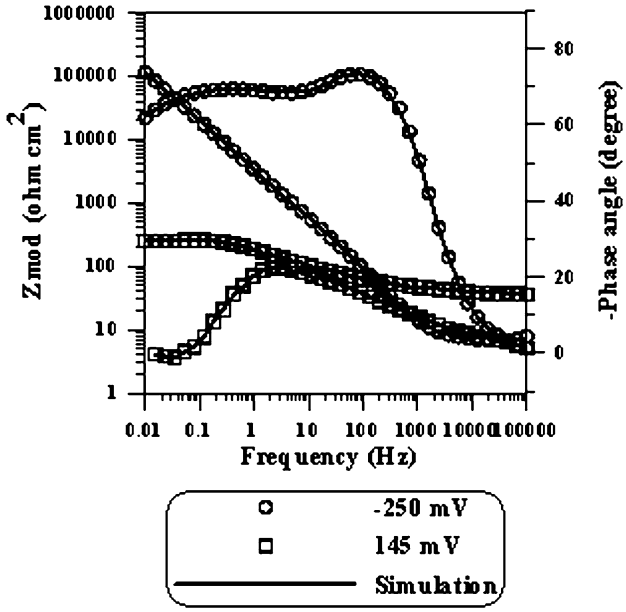

Fig. 9 Bode plots of tested VeraBondV alloy recorded at −250 mV and at 145 mV in acidified artificial saliva at 25 °C

Similar plots were obtained for VeraBondV polarized in acidified artificial saliva at −250 mV as those obtained after 1 week of immersion in acidified artificial saliva (Fig. 7). The best data-fitting EC is similar to EC presented in Fig. 8(a).

The large magnitude of impedance was observed at the passive range of potential. Hence, the resistance of the film in the passive region is still larger ($R_p = 1.25 \times 10^5$ Ω cm^2) than the resistance of the alloy at open-circuit potential after 1-week immersion in acidified artificial saliva ($R_p = 1.29 \times 10^5$ Ω cm^2), accounting for the good corrosion resistance of the alloys.

For the VeraBondV alloys polarized in artificial saliva at 145 mV, within the low-frequency range, an inductive behavior is observed. This behavior is most probably due to the

Table 4 Impedance parameters of VeraBondV alloy in artificial saliva at different potentials

Imposed potential, mV	R_1, Ω cm^2	Q_1, S/cm^2 s^n	n_1	R_2, Ω cm^2	Q_2, S/cm^2 s^n	n_2	L, H/cm^2
−250	15×10^3	2.7×10^{-5}	0.85	1.1×10^5	1.3×10^{-5}	0.83	…
145	242	234×10^{-5}	0.43	210	…	…	231

relaxation process of an intermediate species of the dissolution reaction. In this case the impedance data were fitted with the EC presented in Fig. 8(b), and all the resulting EIS parameters are given in Table 4.

For the VeraBondV alloys polarized in acidified artificial saliva at 145 mV, the value of R_1, representing the charge transfer resistance R_{ct}, is quite low: 242 Ω cm^2. The R_2L element is usually attributed to the relaxation of the corrosion products on the electrode surface (Ref 33, 39). In this case, the protectiveness of oxide film is no longer present. The EIS data are in agreement with the CCP data.

4. Conclusions

The results obtained in this study showed the electrochemical corrosion behavior of the five Ni-based casting dental alloys in acidified artificial saliva (pH 2.3). Owing to their extreme sensitivity to the surface conditions, electrochemical techniques play an indispensable role in evaluating these materials.

The CCP tests of both Ni-Cr alloys with chromium contents (14-18%) indicated the susceptibility to localized corrosion. From the CCP studies, the breakdown potentials for two Ni-Cr-Mo alloys, with higher chromium (22-25%) and molybdenum (9-11%) contents were found to be nobler than those of the Ni-Cr-Mo with chromium (≈13%) and molybdenum (9%) contents. This indicated the beneficial effect of chromium and molybdenum in improving the pitting resistance of Ni-based dental alloys. The Ni-Cr-Mo alloy with chromium (≈13%) and molybdenum (9%) contents presents a dangerous breakdown, but have a sufficiently negative ZCP that the difference between them is around 650 mV. The EIS tests confirm that this Ni-Cr-Mo alloy exhibits passivity after 1-week immersion in acidified artificial saliva, at the open-circuit potential. The breakdown potential from the polarization data is in good agreement with EIS that from the data. The Ni-based casting alloy has pitting-resistant characteristic in acidified artificial saliva when the PRE value increases up to 54.

Acknowledgments

This articles was supported by the project PERFORM-ERA "Postdoctoral Performance for Integration in the European Research Area" (ID-57649), financed by the European Social Fund and the Romanian Government.

References

1. J.R. Davis, *Handbook of Materials for Medical Devices*, ASM International, Materials Park, OH, 2003
2. K.L. Wapner, Implications of Metallic Corrosion in Total Knee Arthroplasty, *Clin. Orthop. Relat. Res.*, 1991, **271**, p 12–20
3. M. Cortada, L.L. Giner, S. Costa, F.J. Gil, D. Rodrigez, and J.A. Planell, Galvanic Corrosion Behaviour of Titanium Implants Coupled to Dental Alloys, *J. Mater. Sci. Mater. Med.*, 2005, **27**, p 1728–1734
4. R. Venugopalan and L.C. Lucas, Evaluation of Restorative and Implant Alloys Galvanically Coupled to Titanium, *Dent. Mater.*, 1998, **14**, p 165–172
5. C.M. Wylie, R.M. Shelton, G.J.P. Fleming, and A.J. Davenport, Corrosion of Nickel-Based Dental Casting Alloys, *Dent. Mater.*, 2007, **23**, p 714–723
6. K.F. Leinfelder, An Evaluation of Casting Alloys Used for Restorative Procedures, *J. Am. Dent. Assoc.*, 1997, **128**, p 37–45
7. R.G. Craig and J.M. Powers, *Restorative Dental Materials*. 11th ed., Mosby Inc (an affiliate of Elsevier Science), 2002
8. W.Z. Friend, *Corrosion of Nickel and Nickel-Based Alloys*, John Wiley and Sons, New York, 1980
9. J. Geis-Gerstorfer and E.H. Greener, Effect of Mo Content and pH Value on the Corrosion Behavior of Ni-20Cr-Mo Dental Alloys, *Dtsch. Zahnarzt. Z.*, 1989, **44**, p 863–866
10. M.A. Ameer, E. Khamis, and M. Al-Motlaq, Electrochemical Behaviour of Recasting Ni-Cr and Co-Cr Non-Precious Dental Alloys, *Corros. Sci.*, 2004, **46**, p 2825–2836
11. D. Mareci, G. Ungureanu, N. Aelenei, and J.C. Mirza Rosca, Comparative Corrosion Study of Non-Precious Ni/Cr-Based Soft Alloys in View of Dental Applications, *Environ. Eng. Manag. J.*, 2008, **7**, p 41–49
12. M. Sharma, A.V. Ramesh Kumar, N. Singh, N. Adya, and B. Saluja, Electrochemical Corrosion Behaviour of Dental/Implant Alloys in Artificial Saliva, *JMEP*, 2008, **17**, p 695–701
13. V.S. Saji and H.C. Choe, Preferential Dissolution Behaviour in Ni-Cr Dental Cast Alloy, *Bull. Mater. Sci.*, 2010, **33**, p 463–468
14. J.D. Bumgardner and L.C. Lucas, Cellular Response to Metallic Ions Released from Nickel-Chromium Dental Alloys, *J. Dent. Res.*, 1995, **74**, p 1521–1527
15. J.D. Bumgardner, J. Doeller, and L.C. Lucas, Effect of Nickel-Based Dental Casting Alloys on Fibroblast Metabolism and Ultrastructural Organization, *J. Biomed. Mater. Res.*, 1995, **29**, p 611–617
16. H.-Y. Lin, B. Bowers, J.T. Wolan, Z. Cai, and J.D. Bumgardner, Metallurgical, Surface, and Corrosion Analysis of Ni-Cr Dental Casting Alloys Before and After Porcelain Firing, *Dent. Mater.*, 2008, **24**, p 378–385
17. J.C. Sectos, A. Babei-Mahani, L. Di Silvio, I.A. Mjor, and N.H.F. Wilson, The Safety of Nickel Containing Dental Alloys: A Review, *Dent. Mater.*, 2006, **22**, p 1163–1168
18. R.I. Holland, Corrosion Testing by Potentiodynamic Polarization in Various Electrolytes, *Dent. Mater.*, 1992, **8**, p 241–245
19. J.F. McCabe, *Applied Dental Materials*, 7th ed., Blackwell Science, Oxford, 1990
20. T. Fusayama, T. Katayori, and S. Nomoto, Corrosion of Gold and Amalgam Placed in Contact with Each Other, *J. Dent. Res.*, 1963, **42**, p 1183–1197
21. G. Airoldi, G. Riva, M. Vanelli, V. Filippi, and G. Garattini, Oral Environment Temperature Changes Induced by Cold/Hot Liquid Intake, *Am. J. Orthod. Dentofac. Orthop.*, 1997, **112**, p 58–63
22. D. Mareci, D. Sutiman, A. Cailean, and J.C. Mirza Rosca, Electrochemical Characterization of Some Dental Materials in Accelerated Environmental Testing, *Environ. Eng. Manag. J.*, 2009, **8**, p 397–407
23. A. Kawashima, K. Asami, and K. Hashimoto, XPS Study of Anodic Behavior of Amorphous Nickel-Phosphorus Alloys Containing Chromium, Molybdenum or Tungsten in 1 M HCl, *Corros. Sci.*, 1984, **24**, p 807–823
24. B.E. Wilde and E. Williams, The Use of Current/Voltage Curves for the Study of Localized Corrosion and Passivity Breakdown on Stainless Steels in Chloride Media, *Electrochim. Acta*, 1971, **16**, p 1971–1985
25. J.R. Scully and R.G. Kelly, Methods for Determining Aqueous Corrosion Reaction Rates, *ASM Handbook*, Vol 13A, S.D. Cramer

and B.S. Covino, Jr., Ed., ASM International, Materials Park, OH, 2003
26. G.S. Frankel, Pitting Corrosion, *ASM Handbook*, Vol 13A, S.D. Cramer and B.S. Covino, Jr., Ed., ASM International, Materials Park, OH, 2003
27. J.D. Bumgardner, M. Roach, T. Scheel, and S. Gardner, Corrosion and XPS Surface Evaluation of Nickel-Chromium Based Dental Casting Alloys, *South Biomed. Eng. Conf. Proc.*, IEEE, 1998
28. J.D. Bumgardner and L.C. Lucas, Surface Analysis of Nickel Chromium Dental Alloys, *Dent. Mater.*, 1993, **9**, p 252–259
29. M. Roach, D. Parsell, S. Gardner, and J.D. Bumgardner, Correlation of Corrosion and Surface Analyses for Ni-Cr Alloys, *Crit. Rev. Biomed. Eng.*, 1998, **26**, p 391–392
30. H.H. Huang, Effect of Chemical Composition on the Corrosion Behaviour of Ni-Cr-Mo Dental Casting Alloys, *J. Biomed. Mater. Res.*, 2002, **60**, p 458–465
31. T.J. Glover, Recent Developments in Corrosion-Resistant Metallic Alloys for Construction of Seawater Pumps, *Mater. Perform.*, 1988, **27**, p 51–56
32. G. Rondelli and B. Vicentini, Effect of Copper on the Localized Corrosion Resistance of Ni-Ti Shape Memory Alloy, *Biomaterials*, 2002, **23**, p 639–644
33. M. Meticos-Hukovic, Z. Pilic, R. Babic, and D. Omanovic, Influence of Alloying Elements on the Corrosion Stability of CoCrMo Implant Alloy in Hank's Solution, *Acta Biomater.*, 2006, **2**, p 693–700
34. T.P. Moffat and R.M. Latanision, An Electrochemical and X-ray Photoelectron Spectroscopy Study of the Passive State of Chromium, *J. Electrochem. Soc.*, 1992, **139**, p 1869–1879
35. S. Haupt and H.H. Strehblow, Combined Electrochemical and Surface Analytical Investigations of the Formation of Passive Layers, *Corros. Sci.*, 1989, **29**, p 163–182
36. E.B. Castro and J.R. Vilche, Investigation of Passive Layer on Iron and Iron-Chromium Alloys by Electrochemical Impedance Spectroscopy, *Electrochim. Acta*, 1993, **38**, p 1567–1572
37. C. Gabrielli, *Identification of Electrochemical Processes by Frequency Response Analysis*, Technical Report Number 004/83, Solartron Instruments, 1983
38. F. Mansfeld, Simultaneous Determination of Instantaneous Corrosion Rates and Tafel Slopes from Polarization Resistance Measurements, *J. Electrochem. Soc.*, 1973, **120**, p 515–518
39. S. Nagarajan, S. Tamilselvi, and N. Rajendran, Evaluation of Localised Corrosion Behaviour of Super Austenitic Stainless Steels Using Dynamic Electrochemical Impedance Spectroscopy, *Mater. Corros.*, 2007, **58**, p 33–38